

Unlabeled sensing with local permutations

Ahmed Ali Abbasi, Abiy Tasissa, Shuchin Aeron

Unlabeled sensing is a linear inverse problem where the measurements are scrambled under an unknown permutation leading to loss of correspondence between the measurements and the rows of the sensing matrix. Motivated by practical tasks such as mobile sensor networks, target tracking and the pose and correspondence estimation between point clouds, we study a special case of this problem restricting the class of permutations to be local and allowing for multiple views. In this setting, namely unlabeled multi-view sensing with local permutation, previous results and algorithms are not directly applicable. In this paper, we propose a computationally efficient algorithm that creatively exploits the machinery of graph alignment and Gromov-Wasserstein alignment and leverages the multiple views to estimate the local permutations. Simulation results on synthetic data sets indicate that the proposed algorithm is scalable and applicable to the challenging regimes of low to moderate SNR.

Index Terms—Graph Matching, Gromov-Wasserstein Alignment, Multi-view, Sliced Gromov-Wasserstein, Unlabeled Sensing

I. INTRODUCTION

Motivated by several practical problems such as sampling in the presence of clock jitter, mobile sensor networks and multiple target tracking in radar, the problem of unlabeled sensing was first considered in [1]. There, the authors derived information theoretic results for identification of unknown signal under linear measurements when the measurement correspondence is lost. Several generalizations of this problem as well as specific cases have been considered in [2]–[13]. A detailed survey of these works vis-a-vis our work is outlined in the related work section I-B. Below we want to first introduce and motivate the model considered here.

In this paper, we study a specific case of this problem where the set of permutations, modeling the loss of correspondence, is local. Specifically, we consider the following task: Estimate the unknown signal $\mathbf{X}^* \in \mathbb{R}^{d \times m}$ from the views $\mathbf{Y} \in \mathbb{R}^{n \times m}$ such that

$$\mathbf{Y} = \mathbf{\Pi}_r^* \mathbf{B} \mathbf{X}^* + \mathbf{N}. \quad (1)$$

In the representation above, $\mathbf{B} \in \mathbb{R}^{n \times d}$ is the known measurement matrix, $\mathbf{N} \in \mathbb{R}^{n \times m}$ is additive noise with i.i.d entries from the Gaussian distribution $\mathcal{N}(0, \sigma^2)$ and $\mathbf{\Pi}_r^* \in \mathbb{R}^{n \times n}$ is an r -local permutation defined below.

Definition 1: Permutation $\mathbf{\Pi}_r \in \mathbb{R}^{n \times n}$ is r -local, i.e. $\mathbf{\Pi}_r \in \mathbb{P}_r$, if it is composed of n/r blocks along the diagonal, with each block being a permutation matrix of size $r \times r$. More precisely, $\mathbf{\Pi}_r$ is a block diagonal matrix, $\mathbf{\Pi}_r = \text{diag}(\pi_1, \dots, \pi_{n/r})$ where π_i denotes the i -th block $r \times r$ permutation matrix.

Fig. 1 shows examples of r -local permutations for $r = 20$.

A. Motivating Applications

While there may be several applications that can fall under the proposed model, here we outline (a) sampling in the presence of timing jitter and (b) the pose and correspondence problem between point clouds. For the first application, consider samples $y(i) = x(iT)$ of an analog signal $x(t)$. Jittered sampling [14] defined as $y(i) = x(iT + T_{\text{skew}})$ in interleaved

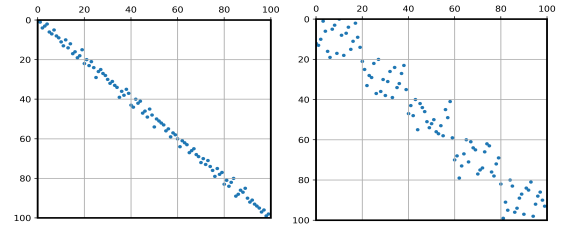


Fig. 1: Left: The sparse permutation with r -local structure considered in [11] with $r = 20$. A permutation is sparse [10] if it has a small number of off diagonal elements. Right: 20-local permutation without sparsity.

ADC systems [15] scrambles the order of the r samples output at each cycle. Fig. 2 illustrates this application. The second application is the pose and correspondence problem which has applications in image processing and computer graphics [9], [16], [17]. The problem considers the alignment of two point clouds given that one of the point clouds is a linear transformation of the other. In addition, the correspondence between few landmarks/keypoints of the point clouds is scrambled via an unknown permutation. Fig. 3 illustrates this application.

B. Relation to Existing Work

The problem of unlabeled sensing has received considerable attention. In addition to the fully shuffled case, several variants with structure on either \mathbf{X}^* and/or the underlying permutation $\mathbf{\Pi}^*$ have been studied. The single view case is a specific instance of the problem in (1), with $m = 1$, where the view matrix \mathbf{Y} reduces to a single column vector. In particular, the model equation is $\mathbf{y} = \mathbf{\Pi}_r^* \mathbf{B} \mathbf{x}^* + \mathbf{n}$ where \mathbf{x}^* and \mathbf{n} denote the signal vector and noise vector respectively. For the single view unlabeled sensing problem, without imposing any extra structure on $\mathbf{\Pi}^*$ or on \mathbf{x}^* , the work in [4] employs symmetric polynomials with degree $d!$ to characterize the unknown permutation and formulates the signal recovery problem as solving a system of polynomial equations. In [2], the underlying permutation is treated as a hidden variable and the likelihood of the observations \mathbf{y} is maximized using the expectation-maximization (EM) approach. The authors in [3] develop an algebraic theoretic framework for the single

The authors are with Tufts University, Medford, USA e-mail:ahmed.abbasi@tufts.edu

This research is supported by NSF CCF:1553075, NSF TRIPODS grant HDR:1934553, and AFOSR FA9550-18-1-0465.

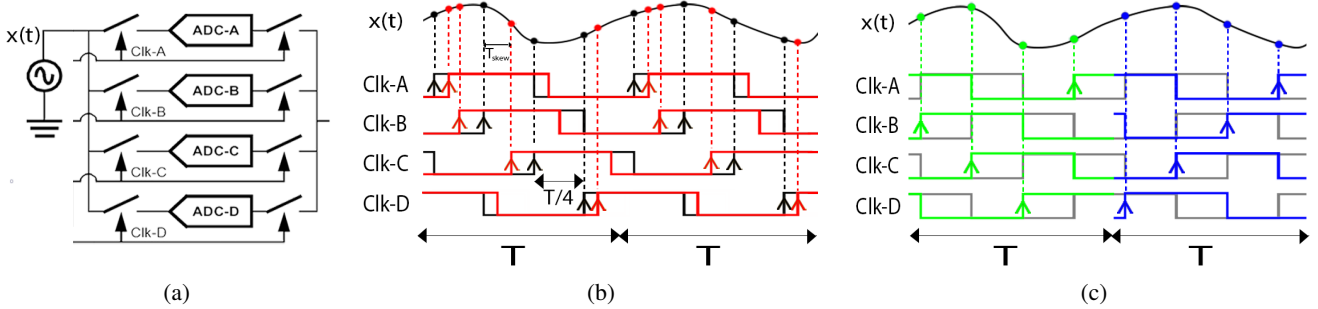


Fig. 2: Left. Interleaved ADC sampling scheme of order 4. At each clock cycle T , 4 samples, $y(i)$ of input signal, $x(t)$ are output as $y(i) = x(i \cdot (T/4)) \forall i \in [4]$. Middle. Red: Jittered Sampling, Jittered samples $y(i) = x(i \cdot (T/4) + T_{\text{skew}})$. Black: Ideal samples, without skew, at time indices, $t_i = i \cdot (T/4)$. Right. Unlabeled Sampling, Correspondence within each cycle (green, blue) of 4 samples, y_1, y_2 is lost: $y_1(i) = x(\pi_1(i) \cdot (T/4))$, $y_2(i) = x(\pi_2(i) \cdot (T/4))$.

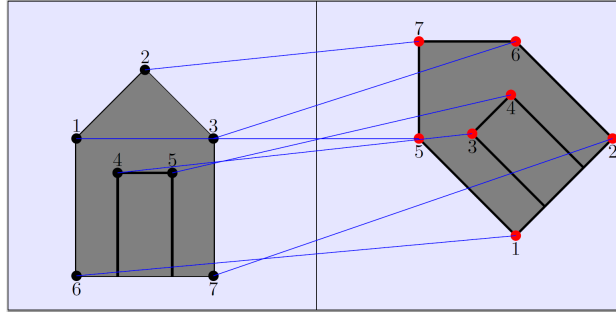


Fig. 3: Left: An object with 7 keypoints, Right: The object after linear transformation (a rotation of 45 degrees) with 7 keypoints. In the pose and correspondence problem, given the keypoints corresponding to the left and right images, the task is to find the underlying permutation.

view unlabeled sensing problem and generalize a dynamic programming algorithm first proposed in [18] for an ordered selection to the fully shuffled case. In [7], an algorithm based on lattice reduction was proposed for the case when the entries of the signal x are picked i.i.d from the normal distribution. The main result therein holds for a fixed signal x^* i.e. the result is not universal for all signals. In addition, the proposed algorithm is mainly for theoretical analysis and is not intended as a feasible practical method. [8] considers a sparse signal x^* and proposes an efficient branch and bound method to search over the set of permutations.

For the multiview unlabeled sensing problem, the subject of the present paper, the LEVSORT algorithm in [9] recovers the unknown permutation by aligning the leverage scores corresponding to the measurements matrix \mathbf{Y} and sensing matrix \mathbf{B} . A drawback of this algorithm is its sensitivity to additive noise. In [10], another structure on $\mathbf{\Pi}^*$ is considered for the multiview setting, namely that the number of shuffled elements is much smaller compared to n . By observing that the inliers lie in the span of a lower d -dimensional subspace of \mathbb{R}^n , the authors in [10] consider a sparse subspace clustering [19] approach. For the same model proposed in [10], namely sparse $\mathbf{\Pi}^*$, [6], [13] proposed ℓ_1 constrained robust regression formulations based on the insight that enforcing sparsity on \mathbf{X} ignores the mismatched measurements as noise. In addition to assuming structure on the unknown permutation $\mathbf{\Pi}^*$, previous techniques are applicable when dimension d is small [3], [4] and require a high oversampling factor ($n \gg d$). The results

in [9]–[11] require number of views m equal to dimension d . By contrast, we consider recovery under a more challenging regime where n scales moderately with d , a small number of views, $m < d$, and additive measurement noise. Furthermore, unlike [12], we do not decrease variance σ^2 as the number of views m is increased. In particular, for $\mathbf{X} \in \mathbb{R}^{d \times m}$, we let $\sigma^2 = \frac{\|\mathbf{B}\mathbf{X}\|_F^2}{n \cdot \text{SNR}}$ whereas $\sigma^2 = \frac{\|\mathbf{X}\|_F^2}{m \cdot \text{SNR}}$ in [12]. As defined in [12], for a constant SNR, σ^2 decreases with increasing m . Finally, the block diagonal permutation structure we consider has also been discussed in [11] but with the following additional assumptions on the model in (1): (a) The data matrix $\mathbf{X}^* \in \mathbb{R}^{d \times d}$ is orthogonal, (b) The number of views is d , $m = d$ and (c) The unknown block diagonal permutation $\mathbf{\Pi}_r^*$ is sparse in contrast to our model. The discussion in section II shows that the assumptions in [11] result in a simpler instantiation of the graph alignment problem than the one considered in this paper.

a) *Major Contributions:* Our main contributions can be summarized as follows.

- 1) For the unlabeled sensing problem, we present a novel graph matching formulation and propose an algorithm that creatively exploits the machinery of Graph Alignment/Gromov-Wasserstein (GW) to resolve local permutations via multiple views. In contrast to many existing methods, the proposed algorithm is applicable to high dimensions and is shown to be robust to additive noise.
- 2) Motivated by several applications, we analyze a novel permutation model that we refer to as the r -local model

Paper	Model ($\Pi \mid \mathbf{X}_{d \times m} \mid \sigma^2$)	Approach
[2]	$\Pi \in \Pi \mid m = 1 \mid \sigma^2 > 0$	Likelihood Maximization
[3]	$\Pi \in \Pi \mid m = 1 \mid \sigma^2 > 0$	Dynamic Programming
[4]	$\Pi \in \Pi \mid m = 1 \mid \sigma^2 > 0$	Symmetric Polynomials
[5]	$\Pi \in \Pi \mid d = 1, m = 1 \mid \sigma^2 > 0$	One Dimensional Sorting
[6]	$\Pi \in \Pi_o \mid m = 1 \mid \sigma^2 > 0$	Convex Relaxation
[7]	$\Pi \in \Pi \mid m = 1, \text{ fixed } \mathbf{x} \mid \sigma^2 = 0$	Lattice Reduction
[8]	$\Pi \in \Pi \mid m = 1, \text{ sparse } \mathbf{x} \mid \sigma^2 = 0$	Branch and Bound
[9]	$\Pi \in \Pi \mid m = d \mid \sigma^2 = 0$	Subspace Matching
[10]	$\Pi \in \Pi_o \mid m = d \mid \sigma^2 > 0$	Subspace Clustering
[11]	$\Pi \in \Pi_o \cap \Pi_r \mid m = d, \mathbf{X}\mathbf{X}^\top = \mathbf{X}^\top\mathbf{X} = \mathbf{I} \mid \sigma^2 > 0$	Orthogonal Least Squares
[12]	$\Pi \in \Pi \mid m > d \mid \sigma^2 > 0$	Convex Relaxation
[13]	$\Pi \in \Pi_o \mid m > 1 \mid \sigma^2 > 0$	Convex Relaxation
This paper	$\Pi \in \Pi_r \mid m > 1 \mid \sigma^2 > 0$	Graph Matching, Gromov-Wasserstein Alignment

TABLE I: Summary of Existing Works. Π denotes the general set of permutations. Π_o denotes sparse permutations. Π_r , considered in this paper, is the set of r -local permutations.

(see Def. 1). A very restrictive version of the r -local model was considered in [11] and the setup that we consider here significantly expands upon the model therein. Our algorithm is further applicable to more general and challenging regimes than the one considered in [11].

- 3) One of the main conclusions of this paper is the observation that for the r -local model, multiple views significantly help in signal and permutation recovery.

b) Outline: The rest of the paper is organized as follows: Section II outlines our proposed approach. In section III, our proposed algorithm is discussed. In section IV, detailed simulation results are provided. We conclude in Section V with the main findings of the paper.

C. Notation

The following is a summary of the notation used in this paper. Let $\mathbf{b}_i^\top \forall i \in [n]$ denote the rows (measurement vectors) of the matrix $\mathbf{B} \in \mathbb{R}^{n \times d}$ i.e. $\mathbf{B}^\top = [\mathbf{b}_1^\top \mid \dots \mid \mathbf{b}_n^\top]$. Similarly $\mathbf{Y}^\top = [\mathbf{y}_1^\top \mid \dots \mid \mathbf{y}_n^\top]$. Let \mathbf{y}_j denote the columns (views) of the matrix, $\mathbf{Y} \in \mathbb{R}^{n \times m}$ i.e. $\mathbf{Y} = [\mathbf{y}_1 \mid \dots \mid \mathbf{y}_m]$. Let $\mathbf{B}_k \in \mathbb{R}^{r \times d} \forall k \in [n/r]$ denote blocks of \mathbf{B} i.e. $\mathbf{B}^\top = [\mathbf{B}_1^\top \mid \dots \mid \mathbf{B}_{n/r}^\top]$. $\mathbf{y}(q) \in \mathbb{R}$ denotes the q^{th} entry of vector $\mathbf{y} \in \mathbb{R}^n$. Let $\mathcal{P}, \mathcal{Q}, \mathcal{K}$ denote the sets of indices of measurement vectors (rows of \mathbf{B}), measurements (rows of \mathbf{Y}) and n/r blocks respectively i.e. $\mathcal{P} = \mathcal{Q} = \{1, \dots, n\}, \mathcal{K} = \{1, \dots, n/r\}$. Let $k_r = \{(k-1)r+1, \dots, kr\}$. $\mathbf{1}_i \in \mathbb{R}^n$ denotes the vector which is equal to 1 at indices $\{(i-1)r+1, \dots, ir\}$ and 0 otherwise. $\mathbf{1}_r \in \mathbb{R}^r$ denotes the r -dimensional vector of all ones. Π_n denotes the set of permutations in $\mathbb{R}^{n \times n}$. Π_i returns the index of the corresponding non zero element in row i of Π . $\Gamma_{\mathbf{1}_n \times \mathbf{1}_n} \in \mathbb{R}_+^{n \times n}$ is the set of couplings: $\{\Gamma \in \mathbb{R}_+^{n \times n} \mid \sum_{i \in [n]} \Gamma_{i,j} = 1; \sum_{j \in [n]} \Gamma_{i,j} = 1\}$. \mathbf{I} denotes the identity matrix. The Moore-Penrose pseudoinverse of a matrix is denoted by $(\cdot)^\dagger$.

II. PROPOSED APPROACH

Our main idea is to exploit the theory and methods for graph matching, i.e. aligning the nodes of two graphs to maximize similarity between the edges, via solving the so-called Quadratic Assignment Problem (QAP) [20].

Given permuted observations \mathbf{Y} , the sensing matrix \mathbf{B} and with \mathbf{C}_Y and $\mathbf{C}_{\hat{Y}}$ denoting Euclidean distance matrices, the unknown permutation Π^* is estimated as follows.

$$\hat{\Pi}^\top \in \arg \min_{\hat{Y} \in \mathbb{R}^{n \times m}, \Pi \in \Pi} \|\mathbf{C}_Y - \Pi \mathbf{C}_{\hat{Y}} \Pi^\top\|_F^2, \quad (2)$$

where $\hat{Y} = \mathbf{B}\hat{\mathbf{X}}$, $[\mathbf{C}_Y]_{pq} = \|\mathbf{y}_p^\top - \mathbf{y}_q^\top\|^2$ and $[\mathbf{C}_{\hat{Y}}]_{pq} = \|\hat{\mathbf{y}}_p^\top - \hat{\mathbf{y}}_q^\top\|^2$.

For a fixed \hat{Y} , the minimization problem in (2) corresponds to the QAP with adjacency matrices \mathbf{C}_Y and $\mathbf{C}_{\hat{Y}}$. However, unlike the standard QAP [20], where both \mathbf{C}_Y and $\mathbf{C}_{\hat{Y}}$ are known, $\mathbf{C}_{\hat{Y}}$ in (2) has to be estimated as \mathbf{X} is unknown. When \mathbf{X} is orthogonal, as considered in [11], i.e. $\mathbf{X}\mathbf{X}^\top = \mathbf{X}^\top\mathbf{X} = \mathbf{I}$, $\mathbf{C}_{\hat{Y}}$ is independent of the unknown \mathbf{X} . This follows from the invariance of Euclidean similarity matrices under orthogonal transformations. In this case, it is easy to see that the alignment in (2) reduces to,

$$\hat{\Pi}^\top \in \arg \min_{\Pi \in \Pi} \|\mathbf{C}_Y - \Pi \mathbf{C}_B \Pi^\top\|_F^2$$

with $[\mathbf{C}_B]_{pq} = \|\mathbf{b}_p^\top - \mathbf{b}_q^\top\|^2$.

For general \mathbf{X} , we could consider an alternating minimization between $\hat{\Pi}, \hat{\mathbf{X}}$; however, minimizing (2) over Π is an NP-hard problem [20]. To circumvent this, we propose to first estimate $\hat{\mathbf{X}}$, set $\hat{Y} = \mathbf{B}\hat{\mathbf{X}}$ and let $\hat{\Pi}$ be given via a relaxation of (2) as outlined below.

We note that the Euclidean distance matrices $\mathbf{C}_Y, \mathbf{C}_{\hat{Y}}$ can be represented as the sum of m Euclidean distance matrices $\mathbf{C}_{y_j}, \mathbf{C}_{\hat{y}_j}$ where the matrices $\mathbf{C}_{y_j}, \mathbf{C}_{\hat{y}_j}$ are constructed from the columns of \mathbf{Y}, \hat{Y} respectively:

$$[\mathbf{C}_Y]_{pq} = \|\mathbf{y}_p^\top - \mathbf{y}_q^\top\|^2 = \sum_{j=1}^{j=m} (y_p^\top(j) - y_q^\top(j))^2 = \sum_{j=1}^{j=m} [\mathbf{C}_{y_j}]_{pq}$$

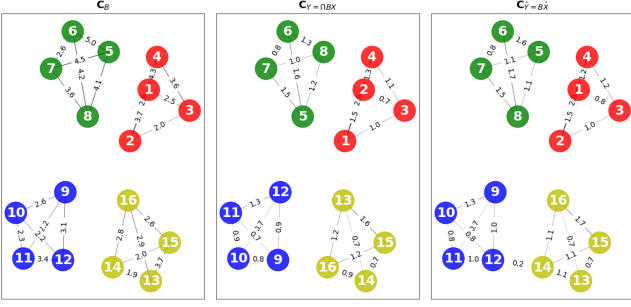


Fig. 4: A block of r consecutive rows in matrices $\mathbf{B}, \mathbf{Y}, \hat{\mathbf{Y}}$ corresponds to a cluster of r nodes in the corresponding graph. Left: The graph of known measurement matrix \mathbf{B} . Middle: The graph of given measurements $\mathbf{Y} = \mathbf{\Pi}^* \mathbf{B} \mathbf{X}$. The r -local permutation, $\mathbf{\Pi}^*$, distorts correspondence of nodes within each cluster, and the unknown linear transformation \mathbf{X} distorts the edge weights. Right: The graph of estimate $\hat{\mathbf{Y}} = \mathbf{B} \hat{\mathbf{X}}$. We first estimate $\hat{\mathbf{Y}}$ and estimate $\mathbf{\Pi}^*$ by matching $\mathbf{C}_{\hat{\mathbf{Y}}}$ to $\mathbf{C}_{\mathbf{Y}}$.

where $[\mathbf{C}_{y_j}]_{pq} = (y_p^\top(j) - y_q^\top(j))^2$. We can restate (2) as:

$$\hat{\mathbf{\Pi}}^\top \in \arg \min_{\hat{\mathbf{Y}} \in \mathbb{R}^{n \times m}, \mathbf{\Pi} \in \mathbb{P}} \left\| \sum_{j=1}^m \mathbf{C}_{y_j} - \mathbf{\Pi} \left(\sum_{j=1}^m \mathbf{C}_{\hat{y}_j} \right) \mathbf{\Pi}^\top \right\|_F^2 \quad (3)$$

We relax (3) by formulating 1-dimensional QAPs between matrices \mathbf{C}_{y_j} and $\mathbf{C}_{\hat{y}_j}$:

$$\hat{\mathbf{P}}_j^\top \in \arg \min_{\hat{y}_j \in \mathbb{R}^n, \mathbf{\Pi} \in \mathbb{P}} \|\mathbf{C}_{y_j} - \mathbf{\Pi} \mathbf{C}_{\hat{y}_j} \mathbf{\Pi}^\top\|_F^2 \quad \forall j \in [m] \quad (4)$$

Our approach is motivated by a recent result for the 1-dimensional QAP. Given $y_j, \hat{y}_j \in \mathbb{R}^n$, the equivalent formulation of (4) reads:

$$\begin{aligned} \hat{\mathbf{P}}_j^\top &\in \arg \max_{\mathbf{\Pi} \in \mathbb{P}} \text{trace}(\mathbf{C}_{y_j} \mathbf{\Pi} \mathbf{C}_{\hat{y}_j}^\top \mathbf{\Pi}^\top) \\ \hat{\mathbf{P}}_j^\top &\in \arg \min_{\mathbf{\Pi} \in \mathbb{P}} \sum_{\substack{p \in [n], \\ q \in [n]}} -(y_j(p) - y_j(q))^2 (\hat{y}_j(\mathbf{\Pi}_p) - \hat{y}_j(\mathbf{\Pi}_q))^2 \end{aligned} \quad (5)$$

For sorted \hat{y}_j, y_j in (5), the optimal assignment is achieved either by the identity or the anti-identity permutation i.e. $\hat{\mathbf{P}}_j^\top \in \{\mathbf{I}, -\mathbf{I}\}$, [21].

We estimate \hat{x}_j from its corresponding view y_j via the following iterations for $y_j, \hat{y}_j, j \in [m]$:

$$\hat{\mathbf{P}}_j^{(t)\top} \in \arg \min_{\mathbf{\Pi} \in \mathbb{P}} \sum_{p,q} -(y_j(p) - y_j(q))^2 (\hat{y}_j^{(t)}(\mathbf{\Pi}_p) - \hat{y}_j^{(t)}(\mathbf{\Pi}_q))^2 \quad (6a)$$

$$\hat{x}_j^{(t+1)} = \mathbf{B}^\dagger (\hat{\mathbf{P}}_j^{(t)\top} y_j) \quad (6b)$$

$$\hat{y}_j^{(t+1)} = \mathbf{B} \hat{x}_j^{(t+1)} \quad (6c)$$

As explained in section III, we leverage the r -local assumption on $\mathbf{\Pi}^*$ to initialize the alternating minimization in (6) via the collapsed linear system of equations (8).

The proposed approach, in addition to alternating minimization between $\hat{x}_j, \hat{\mathbf{P}}_j^\top$, also has a sliced Gromov-Wasserstein [21] based interpretation. Each view $\hat{y}_j^{(t)}, y_j$ is a projection

onto the coordinate axis e_j of the empirical measure $\mu_{\hat{\mathbf{Y}}^{(t)}, \nu_{\mathbf{Y}}}$ supported on the rows of $\hat{\mathbf{Y}}^{(t)}, \mathbf{Y}$ respectively. The alignment in (6a) is then a sliced approximation of the Gromov-Wasserstein distance [22] between Euclidean distance matrices $\mathbf{C}_{\hat{\mathbf{Y}}^{(t)}}, \mathbf{C}_{\mathbf{Y}}$.

Next, we estimate the transpose of the unknown permutation $\mathbf{\Pi}^*$ by minimizing the square of the Gromov-Wasserstein distance [22] between covariance $\mathbf{C}_{\hat{\mathbf{Y}}} = \hat{\mathbf{Y}} \hat{\mathbf{Y}}^\top$, where \hat{y}_j is the estimate from (6), and $\mathbf{C}_{\mathbf{Y}} = \mathbf{Y} \mathbf{Y}^\top$:

$$\text{GW}^2(\mathbf{C}_{\hat{\mathbf{Y}}}, \mathbf{C}_{\mathbf{Y}}) = \min_{\Gamma \in \mathbb{1}} \sum_{p', q'} \sum_{p, q} ([\mathbf{C}_{\hat{\mathbf{Y}}}]_{p'q'} - [\mathbf{C}_{\mathbf{Y}}]_{pq})^2 \Gamma_{p'p} \Gamma_{q'q} \quad (7)$$

where $\mathbb{1}_{n \times n}$ is the set of couplings (or soft permutations) defined in section I-C. (7) is a non-convex optimization problem. We use the algorithm proposed in [23] to solve (7) with entropic regularization. With this perspective, in section III, we propose and outline the algorithm in detail for the r -local permutation model. In section IV, we provide simulation results, and focus particularly on quantifying permutation recovery via the proposed algorithm under an increasing number of views.

III. ALGORITHM

Given sensing matrix \mathbf{B} , locally permuted observations \mathbf{Y} and radius r , we note that, for $\mathbf{X} \in \mathbb{R}^{d \times m}$, each $r \times r$ block of measurement vectors and permuted observations, $[\pi_k \mathbf{B}_k \mid \mathbf{Y}_k] \forall k \in [n/r]$, is an r -dimensional unlabeled sensing problem. We can extract n/r labeled measurements on \mathbf{X} by collapsing each block as below:

$$\begin{aligned} \pi_1 \mathbf{B}_1 \mathbf{X} = \mathbf{Y}_1 &\implies \underbrace{\mathbb{1}_r^\top \pi_1 \mathbf{B}_1}_{\tilde{\mathbf{b}}_1^\top} \mathbf{X} = \underbrace{\mathbb{1}_r^\top \mathbf{Y}_1}_{\tilde{\mathbf{y}}_1^\top} \\ \pi_2 \mathbf{B}_2 \mathbf{X} = \mathbf{Y}_2 &\implies \underbrace{\mathbb{1}_r^\top \pi_2 \mathbf{B}_2}_{\tilde{\mathbf{b}}_2^\top} \mathbf{X} = \underbrace{\mathbb{1}_r^\top \mathbf{Y}_2}_{\tilde{\mathbf{y}}_2^\top} \\ &\vdots \\ \pi_{n/r} \mathbf{B}_{n/r} \mathbf{X} = \mathbf{Y}_{n/r} &\implies \underbrace{\mathbb{1}_r^\top \pi_{n/r} \mathbf{B}_{n/r}}_{\tilde{\mathbf{b}}_{n/r}^\top} \mathbf{X} = \underbrace{\mathbb{1}_r^\top \mathbf{Y}_{n/r}}_{\tilde{\mathbf{y}}_{n/r}^\top} \end{aligned}$$

to form the *collapsed* system:

$$[\tilde{\mathbf{B}} \mid \tilde{\mathbf{Y}}] \in \mathbb{R}^{(n/r) \times m} \quad (8)$$

While the permuted linear system of equations (L.S.E.) $[\mathbf{\Pi}^* \mathbf{B} \mid \mathbf{Y}] \in \mathbb{R}^n$ has $n > d$ permuted measurements, the collapsed L.S.E. $[\tilde{\mathbf{B}} \mid \tilde{\mathbf{Y}}] \in \mathbb{R}^{n/r}$ is under determined with n/r measurements. We consider recovery of $\mathbf{X}, \mathbf{\Pi}$ in the case $d > n/r$.

Stage A of the algorithm iterates over the following for

Algorithm 1 De-permute**Input:** Radius $r \in \mathbb{R}$, $\mathbf{B} \in \mathbb{R}^{n \times d}$, $\mathbf{Y} \in \mathbb{R}^{n \times m}$ **Output:** $\hat{\mathbf{X}}, \hat{\Pi}_r$

// Stage-A

for $j \in 1, \dots, m$ **do** $\mathcal{P} \leftarrow \{1, \dots, n\}, \mathcal{Q} \leftarrow \{1, \dots, n\}, \mathcal{K} \leftarrow \{1, \dots, n/r\}$ $\tilde{\mathbf{b}}_i^{\top(1)} \leftarrow \mathbb{1}_i^{\top} \mathbf{B} \quad \tilde{\mathbf{y}}_i^{\top(1)} \leftarrow \mathbb{1}_i^{\top} \mathbf{Y} \forall i \in [n/r]$ **for** $t \in 1 \dots d - n/r$ **do** $\hat{\mathbf{y}}_j^{(t)} \leftarrow \mathbf{B} \left(\tilde{\mathbf{B}}^{(t)\dagger} \tilde{\mathbf{y}}_j^{(t)} \right)$ **for** $k \in \mathcal{K}^{(t)}$ **do** $\mathcal{P}_k \leftarrow \text{sort}(\hat{\mathbf{y}}_j, k_r \cap \mathcal{P}^{(t)}) \quad \mathcal{Q}_k \leftarrow \text{sort}(\mathbf{y}_j, k_r \cap \mathcal{Q}^{(t)})$ $(p_k, q_k) \in \arg \min_{(p \in \mathcal{P}_k, q \in \mathcal{Q}_k)} \left\| \mathbf{y}_j - \mathbf{B} \left[\frac{\tilde{\mathbf{B}}^{(t)}}{\mathbf{b}_p^{\top}} \right]^{\dagger} \left[\frac{\tilde{\mathbf{y}}_j^{(t)}}{y_j(q)} \right] \right\|_2$ **end for** $k^* \in \arg \min_{(p_k, q_k)} \left\| \mathbf{y}_j - \mathbf{B} \left[\frac{\tilde{\mathbf{B}}^{(t)}}{\mathbf{b}_{p_k}^{\top}} \right]^{\dagger} \left[\frac{\tilde{\mathbf{y}}_j^{(t)}}{y_j(q_k)} \right] \right\|_2$ $\tilde{\mathbf{B}}^{(t+1)} \leftarrow \left[\frac{\tilde{\mathbf{B}}^{(t)}}{\mathbf{b}_{p_k^*}^{\top}} \right] \quad \tilde{\mathbf{y}}_j^{(t+1)} \leftarrow \left[\frac{\tilde{\mathbf{y}}_j^{(t)}}{y_j(q_k^*)} \right]$ $\mathcal{P}^{(t+1)} \leftarrow \mathcal{P}^{(t)} \setminus p_k^* \quad \mathcal{Q}^{(t+1)} \leftarrow \mathcal{Q}^{(t)} \setminus q_k^*$ **if** $(|k_r^* \cap \mathcal{P}_k| == 1)$ $\mathcal{K}^{(t+1)} \leftarrow \mathcal{K}^{(t)} \setminus k^*$ **end if****end for** $\hat{\mathbf{y}}_j \leftarrow \mathbf{B} \left(\tilde{\mathbf{B}}^{(t)\dagger} \tilde{\mathbf{y}}_j^{(t)} \right)$ **end for**

// Stage-B

 $\hat{\pi}_k^{\top} \leftarrow \text{GW}_{\text{threshold}} \left(\hat{\mathbf{Y}}_k \hat{\mathbf{Y}}_k^{\top}, \mathbf{Y} \mathbf{Y}^{\top} \right) \quad \forall k \in [n/r]$ $\hat{\Pi}_r^{\top} = \text{diag} \left(\hat{\pi}_1^{\top}, \dots, \hat{\pi}_{n/r}^{\top} \right)$ $\hat{\mathbf{X}} = \mathbf{B}^{\dagger} \left(\hat{\Pi}_r^{\top} \mathbf{Y} \right)$ $\mathbf{y}_j, \hat{\mathbf{y}}_j, j \in [m]:$

$$\hat{\mathbf{P}}_j^{(t)\top} \in \arg \min_{\Pi \in \Pi_n} \sum_{p,q} - (y_j(p) - y_j(q))^2 \left(\hat{\mathbf{y}}_j^{(t)}(\Pi_p) - \hat{\mathbf{y}}_j^{(t)}(\Pi_q) \right)^2 \quad (9a)$$

$$\tilde{\mathbf{B}}_j^{(t+1)} = \left[\frac{\tilde{\mathbf{B}}_j^{(t)}}{\mathbf{b}_{p^*}^{\top}} \right] \quad \tilde{\mathbf{y}}_j^{(t+1)} = \left[\frac{\tilde{\mathbf{y}}_j^{(t)}}{y_j(q^*)} \right] \quad (9b)$$

$$\hat{\mathbf{y}}_j^{(t+1)} = \mathbf{B} \left(\tilde{\mathbf{B}}_j^{(t+1)\dagger} \tilde{\mathbf{y}}_j^{(t+1)} \right) \quad (9c)$$

$\hat{\mathbf{y}}_j^{(1)}$ in (9) is instantiated by the collapsed system (8) i.e. $\hat{\mathbf{y}}_j^{(1)} = \mathbf{B} \left(\tilde{\mathbf{B}}^{(1)\dagger} \tilde{\mathbf{y}}_j \right)$.

As outlined in section II, (9a) aligns projection $\hat{\mathbf{y}}_j^{(t)}$ to $\mathbf{y}_j^{(t)}$ via the permutation $\hat{\mathbf{P}}_j^{(t)\top}$. Note that $\hat{\mathbf{P}}_j^{(t)\top}$ matches measurement vector \mathbf{b}_p^{\top} to the measurement $y_j(q)$, where q is the non-zero element in row p of $\hat{\mathbf{P}}_j^{(t)}$. Compared to estimating \hat{x}_j as in (6b), (9b) augments the under-determined system $\left[\tilde{\mathbf{B}}^{(t)} \quad \tilde{\mathbf{y}}_j^{(t)} \right]$ by a single (measurement vector, measurement) pair: $(\mathbf{b}_{p^*}^{\top}, y_j(q^*))$. To augment (8) to full-rank, we iterate (9) $d - n/r$ times, where n/r is the number of measurements in the collapsed system (8). In the following, we specialize (9a), (9b) to the r -local model.

As the unknown permutation is r -local i.e., $\Pi_r^* \in \Pi_r$, we match indices (p_k, q_k) within the same block k :

$$\mathcal{P}_k \leftarrow \text{sort}(\hat{\mathbf{y}}_j(k_r)) \quad \mathcal{Q}_k \leftarrow \text{sort}(\mathbf{y}_j(k_r))$$

$$(p_k, q_k) \in \arg \min_{(p \in \mathcal{P}_k, q \in \mathcal{Q}_k)} \left\| \mathbf{y}_j - \mathbf{B} \left[\frac{\tilde{\mathbf{B}}_j^{(t)}}{\mathbf{b}_p^{\top}} \right]^{\dagger} \left[\frac{\tilde{\mathbf{y}}_j^{(t)}}{y_j(q)} \right] \right\|_2$$

$\mathcal{P}_k, \mathcal{Q}_k$ are sorting indices for sub-vectors $\hat{\mathbf{y}}_j(k_r), \mathbf{y}_j(k_r) \in \mathbb{R}^r$ respectively over $k_r = \{(k-1)r+1, \dots, kr\}$. The sorting operation is equivalent to solving the QAP (9a) over each block and picking the identity permutation.

We select indices $(p^{*(t+1)}, q^{*(t+1)})$ such that the forward error $\|\mathbf{y}_j - \hat{\mathbf{y}}^{(t+1)}\|_2$ is minimized:

$$(p^{*(t+1)}, q^{*(t+1)}) \in \arg \min_{(p_k, q_k)} \left\| \mathbf{y}_j - \underbrace{\mathbf{B} \left[\frac{\tilde{\mathbf{B}}_j^{(t)}}{\mathbf{b}_{p_k}^{\top}} \right]^{\dagger} \left[\frac{\tilde{\mathbf{y}}_j^{(t)}}{y_j(q_k)} \right]}_{\hat{\mathbf{y}}_j^{(t+1)}} \right\|_2 \quad (10)$$

The indices $(p^{*(t+1)}, q^{*(t+1)})$ is the pair of indices that minimizes the forward error. As the number of measurements n increases, (10) minimizes the forward error over a larger number of possible pairs.

At each iteration t , we reduce the sets of feasible indices $\mathcal{P}_k, \mathcal{Q}_k$ by excluding indices matched up till iteration $t-1$ from the search:

$$\mathcal{P}^{(t+1)} \leftarrow \mathcal{P}^{(t)} \setminus p^{*(t+1)} \quad \mathcal{Q}^{(t+1)} \leftarrow \mathcal{Q}^{(t)} \setminus q^{*(t+1)}$$

If $r-1$ indices of a block of size r have been matched, we also exclude the single remaining index in that block:

$$\mathbf{if} \left(|k_r \cap \mathcal{P}^{(t+1)}| == 1 \right) \mathcal{K}^{(t+1)} \leftarrow \mathcal{K}^{(t)} \setminus k$$

where $\mathcal{K} = \{1, \dots, n/r\}$ is the set of block indices.

After iterating (9) as described, **Stage B** of the algorithm aligns the blocks $\hat{\mathbf{Y}}_k \hat{\mathbf{Y}}_k^{\top} \in \mathbb{R}^{r \times r}$ with $\mathbf{Y}_k \mathbf{Y}_k^{\top}$ via the Gromov-Wasserstein entropically regularized algorithm:

$$\hat{\Gamma}_k^{\top} = \text{GW}_{\epsilon} \left(\hat{\mathbf{Y}}_k \hat{\mathbf{Y}}_k^{\top}, \mathbf{Y}_k \mathbf{Y}_k^{\top} \right) \forall k \in [n/r]$$

The GW_{ϵ} algorithm outputs a soft coupling, $\hat{\Gamma}_k$. We threshold $\hat{\Gamma}_k$ to obtain permutation $\hat{\pi}_k$. We estimate Π_r^* as:

$$\hat{\Pi}_r^{\top} = \text{diag} \left(\hat{\pi}_1^{\top}, \dots, \hat{\pi}_{n/r}^{\top} \right)$$

In the next section, we evaluate the performance of the algorithm on synthetic datasets. The code to reproduce all the experiments is available at <https://github.com/aabbas02/unlabeled-sensing>.

IV. RESULTS AND PERFORMANCE

For the model in (1), we draw entries of the measurement matrix $\mathbf{B} \in \mathbb{R}^{n \times d}$ and the signal $\mathbf{X}^* \in \mathbb{R}^{d \times m}$ i.i.d from the standard normal distribution. The additive noise \mathbf{N} is drawn i.i.d from Gaussian distribution $\mathcal{N}(0, \sigma^2)$, and the permutation Π_r^* is picked uniformly at random. For all simulations, we set signal dimension $d = 64$, and the $\text{SNR} = \frac{\|\mathbf{B}\mathbf{X}^*\|_F^2}{n\sigma^2} = 30$ db. All results are averaged over 25 Monte Carlo runs.

In Fig. 5, we evaluate the performance of the 1-dimensional QAP based alignment approach in (6). As highlighted in section II, the covariance \mathbf{C}_{Y^*} , where $\mathbf{Y}^* = \mathbf{B}\mathbf{X}^*$, is unknown. We plot the error in our estimate of the covariance $\mathbf{C}_{\hat{Y}}$, where \hat{Y} is given by (6), against the number of views m in Fig. 5. We observe from Fig. 5a that the normalized error decreases as the number of views m is increased. We conclude therefore that the proposed approach is able to exploit multiple views to improve estimate $\mathbf{C}_{\hat{Y}}$. From Fig. 5b, we observe that, for a fixed value of m , the error in $\mathbf{C}_{\hat{Y}}$ increases as the block size r is increased. Recall that for the r -local model in (1) with n measurements, the collapsed system in (8) has n/r measurements. The increased error can be explained by noting that i) n/r decreases as r increases so that the initialization to (6), $\hat{\mathbf{X}}^{(1)}$, is estimated from a decreasing number of measurements ii) the permutation becomes less local as block size r is increased.

In Fig. 6. (a - d), for block size $r \in \{7, 8, 9, 10\}$, we plot the fractional Hamming distortion $d_H(\mathbf{\Pi}_r^*, \hat{\mathbf{\Pi}}_r)/n$ against measurements $n_r = \{48r, 52r, 56r, 60r\}$. We observe from the plots that for all r , the distortion d_H is lower for larger m . Improved performance under larger m can be explained from i) the results in Fig. 5 i.e. the estimate of the covariance of unpermuted observations $\mathbf{C}_{\hat{Y}}$ has lower error with increasing m ii) multiple views offset the effect of additive noise as the required SNR for recovery decreases with increasing views [9], [10], [12]. We observe also that the distortion d_H decreases with increasing measurements n . Recall that the collapsed system in (8) is under-determined by $d - n/r$ measurements, e.g., when $n = 48r$, (8) has 48 measurements and is under-determined by $64 - 48 = 16$ measurements. Lower distortion with increasing n follows from noting that the initialization to (6), $\hat{\mathbf{X}}^{(1)}$, is estimated from an increasing number of measurements as n increases.

In Fig. 6. (e - h), we set the number of views equal to dimension of the signal, $m = d$, and compare our proposed algorithm to an r -local variant of the LEVSORT algorithm proposed in [9]. The LEVSORT algorithm estimates the unknown permutation by matching $\mathbf{U}_B \mathbf{U}_B^T$, where \mathbf{U}_B is the subspace spanned by the left singular vectors of the measurement matrix \mathbf{B} , to $\mathbf{U}_Y \mathbf{U}_Y^T$. Notably, the LEVSORT algorithm, unlike the proposed approach, does not alternate estimation between \mathbf{X} and $\mathbf{\Pi}$. We attribute the better performance of our approach to the alternating estimation procedure in Stage-A of the proposed algorithm.

V. CONCLUSION

We study a linear inverse problem with scrambled measurements well known as the unlabeled sensing problem. In this paper, we focus on a novel setup of this problem, the r -local model, that considers local permutations. We propose an algorithm based on graph matching and Gromov-Wasserstein alignment. Numerical experiments on synthetic data show that the proposed algorithm is robust to additive noise and exploits multiple views for improved recovery.

REFERENCES

- [1] Jayakrishnan Unnikrishnan, Saeid Haghghatshoar, and Martin Vetterli. Unlabeled sensing with random linear measurements. *IEEE Transactions on Information Theory*, 64(5):3237–3253, 2018.
- [2] Abubakar Abid and James Zou. A stochastic expectation-maximization approach to shuffled linear regression. In *2018 56th Annual Allerton Conference on Communication, Control, and Computing (Allerton)*, pages 470–477. IEEE, 2018.
- [3] Manolis Tsakiris and Liangzu Peng. Homomorphic sensing. In Kamalika Chaudhuri and Ruslan Salakhutdinov, editors, *Proceedings of the 36th International Conference on Machine Learning*, volume 97 of *Proceedings of Machine Learning Research*, pages 6335–6344, Long Beach, California, USA, 09–15 Jun 2019. PMLR.
- [4] M. C. Tsakiris, L. Peng, A. Conca, L. Kneip, Y. Shi, and H. Choi. An algebraic-geometric approach for linear regression without correspondences. *IEEE Transactions on Information Theory*, pages 1–1, 2020.
- [5] A. Pananjady, M. J. Wainwright, and T. A. Courtade. Linear regression with shuffled data: Statistical and computational limits of permutation recovery. *IEEE Transactions on Information Theory*, 64(5):3286–3300, 2018.
- [6] Martin Slawski and Emanuel Ben-David. Linear regression with sparsely permuted data. *Electron. J. Statist.*, 13(1):1–36, 2019.
- [7] Daniel J Hsu, Kevin Shi, and Xiaorui Sun. Linear regression without correspondence. In *Advances in Neural Information Processing Systems*, pages 1531–1540, 2017.
- [8] V. Emiya, A. Bonnefoy, L. Daudet, and R. Gribonval. Compressed sensing with unknown sensor permutation. In *2014 IEEE International Conference on Acoustics, Speech and Signal Processing (ICASSP)*, pages 1040–1044, 2014.
- [9] A. Pananjady, M. J. Wainwright, and T. A. Courtade. Denoising linear models with permuted data. In *2017 IEEE International Symposium on Information Theory (ISIT)*, pages 446–450, 2017.
- [10] Martin Slawski, Mostafa Rahmani, and Ping Li. A sparse representation-based approach to linear regression with partially shuffled labels.
- [11] Xu Shi, Xiaoou Li, and Tianxi Cai. Spherical regression under mismatch corruption with application to automated knowledge translation. *Journal of the American Statistical Association*, (just-accepted):1–28, 2020.
- [12] Hang Zhang, Martin Slawski, and Ping Li. Permutation recovery from multiple measurement vectors in unlabeled sensing. In *2019 IEEE International Symposium on Information Theory (ISIT)*, pages 1857–1861. IEEE, 2019.
- [13] Martin Slawski, Emanuel Ben-David, and Ping Li. A two-stage approach to multivariate linear regression with sparsely mismatched data. *CoRR*, abs/1907.07148, 2019.
- [14] A. Balakrishnan. On the problem of time jitter in sampling. *IRE Transactions on Information Theory*, 8(3):226–236, 1962.
- [15] B. Razavi. Design Considerations for Interleaved ADCs. *IEEE Journal of Solid-State Circuits*, 48(8):1806–1817, Aug 2013.
- [16] Steve Mann. Compositing multiple pictures of the same scene. In *Proc. IS&T Annual Meeting, 1993*, pages 50–52, 1993.
- [17] Manuel Marques, Marko Stošić, and João Costeira. Subspace matching: Unique solution to point matching with geometric constraints. In *2009 IEEE 12th International Conference on Computer Vision*, pages 1288–1294. IEEE.
- [18] Saeid Haghghatshoar and Giuseppe Caire. Signal recovery from unlabeled samples. *IEEE Transactions on Signal Processing*, 66(5):1242–1257, Mar 2018.
- [19] Ehsan Elhamifar and Rene Vidal. Sparse subspace clustering: Algorithm, theory, and applications. *IEEE transactions on pattern analysis and machine intelligence*, 35(11):2765–2781, 2013.
- [20] Eliane Maria Loiola, Nair Maria Maia de Abreu, Paulo Oswaldo Boaventura-Netto, Peter Hahn, and Tania Querido. A survey for the quadratic assignment problem. *European Journal of Operational Research*, 176(2):657–690, 2007.
- [21] Vayer Titouan, Rémi Flamary, Nicolas Courty, Romain Tavenard, and Laetitia Chapel. Sliced gromov-wasserstein. In *Advances in Neural Information Processing Systems*, pages 14726–14736, 2019.
- [22] Facundo Mémoli. Gromov-wasserstein distances and the metric approach to object matching. *Foundations of computational mathematics*, 11(4):417–487, 2011.
- [23] Gabriel Peyré, Marco Cuturi, and Justin Solomon. Gromov-wasserstein averaging of kernel and distance matrices. In *International Conference on Machine Learning*, pages 2664–2672, 2016.

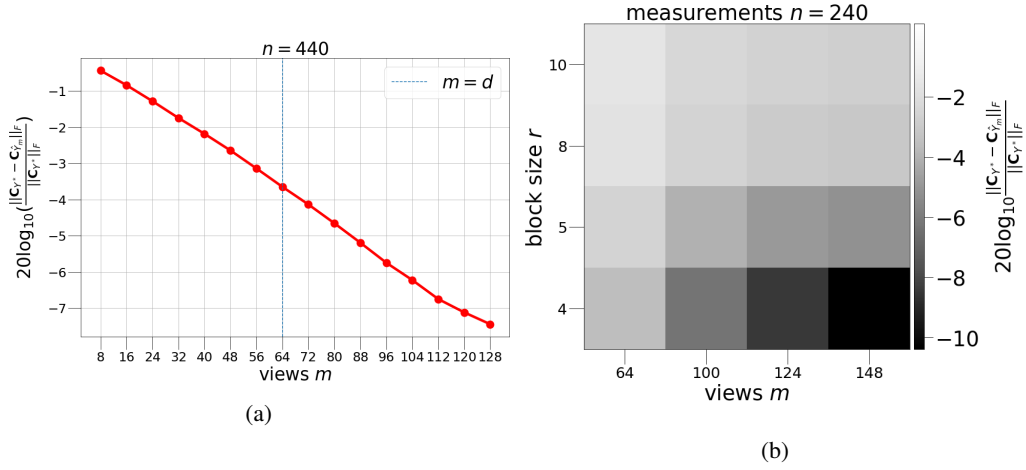


Fig. 5: Figure plots the normalized error in the estimated covariance $\mathbf{C}_{\hat{Y}} = \hat{\mathbf{Y}}\hat{\mathbf{Y}}^\top$ against number of views m for fixed block size $r = 8$ (left) and $r \in \{4, 5, 8, 10\}$ (right).

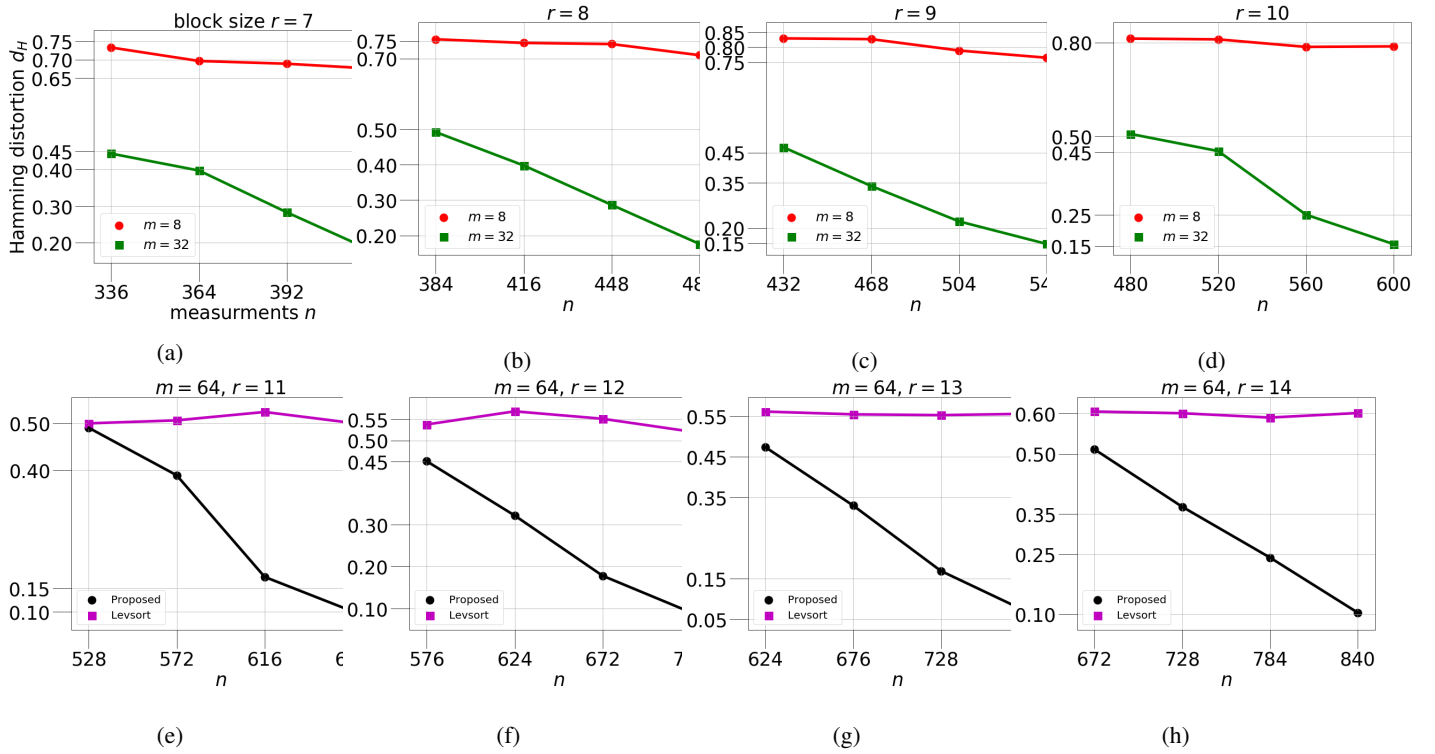


Fig. 6: $\mathbf{Y} = \mathbf{\Pi}_r^* \mathbf{B}_{n \times d} \mathbf{X}_{d \times m}^* + \mathbf{N}$. (a) - (d). For block size $r \in \{7, 8, 9, 10\}$, views $m \in \{8, 32\}$, figure plots the fractional Hamming distortion, $d_H(\mathbf{\Pi}_r^*, \hat{\mathbf{\Pi}}_r)/n$, against measurements n . (e) - (h). For fixed $m = 64$, figure compares distortion in estimate via proposed algorithm to that of block wise LEVSORT [9] for $r \in \{11, 12, 13, 14\}$.